Geophysical Research Letters

RESEARCH LETTER
10.1029/2019GL084053

Key Points:
- Thick cratonic lithosphere extends beneath the Rehoboth Province and parts of the northern Okwa Terrane and Magondi Belt
- The northern edge of the greater Kalahari Craton lithosphere lies along the northern boundary of the Rehoboth Province and Magondi Belt
- Cratonic mantle lithosphere beneath the Okwa Terrane and Magondi Belt may have been chemically altered by Proterozoic magmatic events

Supporting Information:
- Supporting Information S1

Correspondence to:
A. Nyblade,
aan2@psu.edu

Citation:
Ortiz, K., Nyblade, A., van der Meijde, M., Paulssen, H., Kwadiba, M., Ntibinyane, O., et al. (2019). Upper mantle *P* and S wave velocity structure of the Kalahari Craton and surrounding Proterozoic terranes, southern Africa. *Geophysical Research Letters*, *46*, 9509–9518. https://doi.org/10.1029/2019GL084053

Received 11 JUN 2019
Accepted 8 AUG 2019
Accepted article online 16 AUG 2019
Published online 23 AUG 2019

Upper Mantle *P* and *S* Wave Velocity Structure of the Kalahari Craton and Surrounding Proterozoic Terranes, Southern Africa

Kameron Ortiz[1], Andrew Nyblade[1,5], Mark van der Meijde[2], Hanneke Paulssen[3], Motsamai Kwadiba[4], Onkgopotse Ntibinyane[4], Raymond Durrheim[5], Islam Fadel[2,6], and Kyle Homman[1]

[1]Department of Geosciences, Pennsylvania State University, University Park, PA, USA, [2]Faculty for Geo-information Science and Earth Observation (ITC), University of Twente, Enschede, Netherlands, [3]Department of Earth Sciences, Faculty of Geosciences, Utrecht University, Utrecht, Netherlands, [4]Botswana Geoscience Institute, Lobatse, Botswana, [5]School of Geosciences, The University of the Witwatersrand, Johannesburg, South Africa, [6]Geology Department, Faculty of Science, Helwan University, Ain Helwan, Egypt

Abstract New broadband seismic data from Botswana and South Africa have been combined with existing data from the region to develop improved *P* and *S* wave velocity models for investigating the upper mantle structure of southern Africa. Higher craton-like velocities are imaged beneath the Rehoboth Province and parts of the northern Okwa Terrane and the Magondi Belt, indicating that the northern edge of the greater Kalahari Craton lithosphere lies along the northern boundary of these terranes. Lower off-craton velocities are imaged beneath the Damara-Ghanzi-Chobe Belt, and may in part reflect thinning of the lithosphere beneath the incipient Okavango Rift. Lower velocities are also imaged to the north and northwest of the Bushveld Complex beneath parts of the Okwa Terrane, Magondi Belt, and Limpopo Belt, indicating that cratonic upper mantle in some areas beneath these terranes may have been modified by the 2.05-Ga Bushveld and/or 1.1-Ga Umkondo magmatic events.

Plain Language Summary *P* and *S* waves travel times from large, distant earthquakes recorded on seismic stations in Botswana and South Africa have been combined with existing data from the region to construct velocity models of the upper mantle beneath southern Africa. The models show a region of higher velocities beneath the Rehoboth Province and parts of the northern Okwa Terrane and the Magondi Belt, which can be attributed to thicker cratonic lithosphere, and a region of lower velocities beneath the Damara-Ghanzi-Chobe Belt and Okavango Rift, which can be attributed a region of thinner off-craton lithosphere. This finding suggests that the spatial extent of thick cratonic lithosphere in southern Africa is greater than previously known. In addition, within the cratonic lithosphere an area of lower velocities is imaged, revealing parts of the cratonic lithosphere that may have been modified by younger magmatic events.

1. Introduction

The greater Kalahari Craton in southern Africa is commonly regarded as an archetypal Archean terrane, and thus, its structure and tectonic evolution have long been studied to learn about tectonic processes during the first two billion years of Earth history (e.g., Begg et al., 2009; Carlson et al., 2000; Corner & Durrheim, 2018; Griffin et al., 2003; Hartnady et al., 1985). However, much remains unknown about the craton, including its geographic size, defined by the presence of thick lithosphere, and the extent to which the lithosphere may have been modified by Proterozoic magmatic events. For example, does thick (>~150 km) lithosphere extend beneath younger terranes surrounding the craton nucleus, such as the Rehoboth Province, Okwa Terrane, and Magondi Belt (Figure 1; e.g., Corner & Durrheim, 2018; Khoza et al., 2013; Eglington & Armstrong, 2004; Griffin et al., 2003)? And how effective have large magmatic events, such as the Bushveld event, been at modifying the composition and structure of the cratonic lithosphere (e.g., Grégoire et al., 2005; Richardson & Shirey, 2008; Viljoen et al., 2009)?

To address these questions, we have developed *P* and *S* wave velocity models of the upper mantle beneath southern Africa by combining new seismic data from Botswana and South Africa with data from permanent

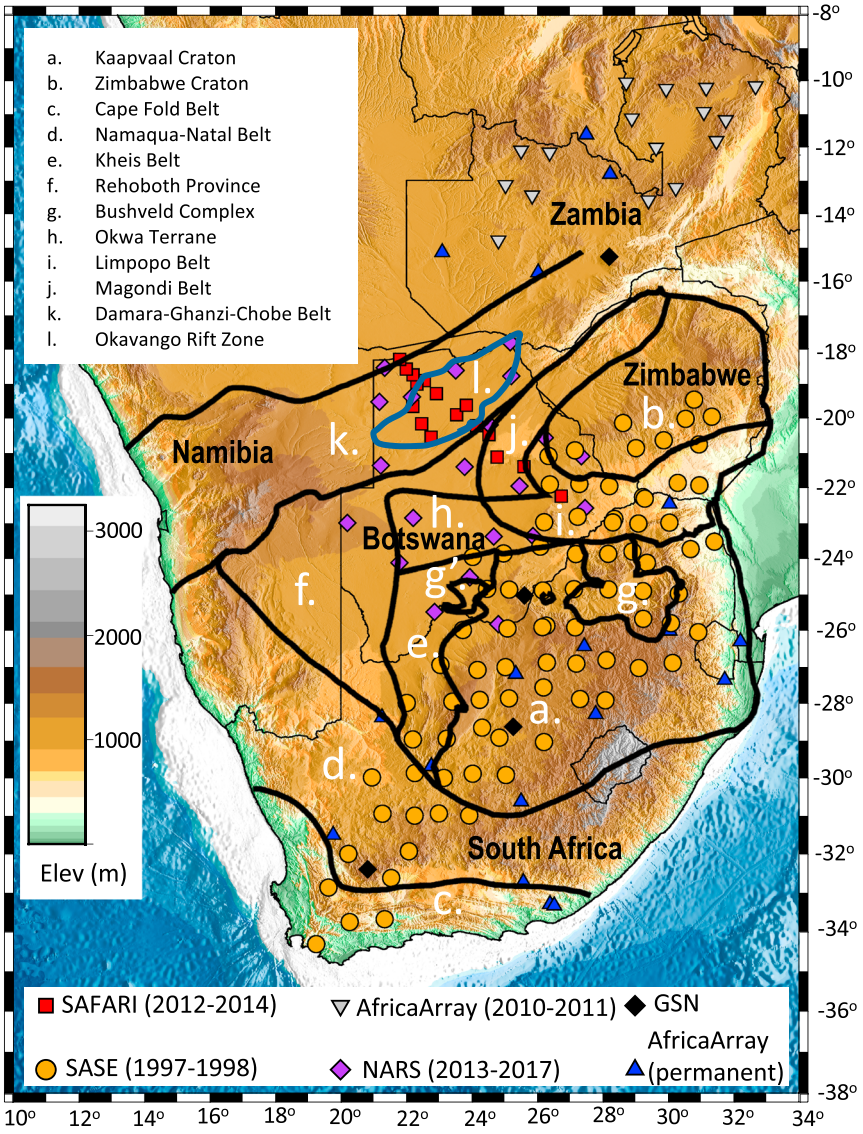

Figure 1. (a–l) Topographic map of the study area showing seismic station locations and tectonic terranes. A description of the seismic networks listed at the bottom of the figure is given in the text. Black lines denote Precambrian terrane boundaries and the blue line denotes the Cenozoic Okavango Rift. The small region labeled g′ is the Malopo Farm Complex, which is part of the Bushveld Complex.

seismic stations and previous temporary seismic deployments in the region. Our models provide new insights into both the structure of the cratonic lithosphere in southern Africa and its composition.

2. Background

2.1. Tectonic Overview

The lithosphere in the study area is composed of several Archean and Proterozoic terranes (Figure 1). The greater Kalahari Craton is composed of the Archean Kaapvaal (Figure 1a) and Zimbabwe (Figure 1b) cratons sutured together by the Archean and Paleoproterozoic Limpopo Belt (Figure 1i; Corner & Durrheim, 2018; de Wit et al., 1992; Dirks & Jelsma, 2002). The Kalahari Craton is bounded to the northwest by the Paleoproterozoic Okwa Terrane (Figure 1h) and Magondi Belt (Figure 1j), and to the south and southwest by the Mesoproterozoic Namaqua-Natal Belt (Figure 1d). The Namaqua sector is separated from the western border of the Kaapvaal Craton by a passive margin sequence referred to as the Kheis Province (Figure 1e;

Cornell et al., 2006; Thomas et al., 1993). The Paleoproterozoic Rehoboth Province (Figure 1f) extends from central and southwestern Botswana to western Namibia outboard of the Kheis Province (Van Schijndel et al., 2011). The Bushveld Complex (2.05 Ga; Figure 1g) extends >350 km north-south and east-west across the northern Kaapvaal Craton (e.g., Cawthorn et al., 2006; Webb et al., 2004) and includes satellite intrusions to the west as far as the Molopo Farms Complex (Figure 1g′) in Botswana (Reichhardt, 1994). The northern part of the study area includes the Damara-Ghanzi-Chobe Belt (Figure 1k), which formed during the Neoproterozoic Pan-African tectono-thermal event (870–550 Ma) when the Kalahari and Congo cratons collided (Kröner & Stern, 2004). The Okavango Rift Zone (ORZ; Figure 1l) is located within the Damara-Ghanzi Chobe Belt, and is considered an incipient rift system (Kinabo et al., 2008; Modisi et al., 2000). At the southern end of the study area, the Paleozoic Cape Fold Belt (Figure 1c) formed outboard of the Namaqua-Natal Belt.

2.2. Previous Seismic Studies

A large number of seismic studies have investigated crust and mantle structure in southern Africa over the past few decades using body wave tomography (e.g., Fouch et al., 2004; Youssof et al., 2015; Yu et al., 2016), surface wave tomography (e.g., Chevrot & Zhao, 2007; Priestley et al., 2008; Fishwick, 2010; Adams & Nyblade, 2011), receiver functions (e.g., Fadel et al., 2018; Hansen et al., 2009; Kgaswane et al., 2009; Nguuri et al., 2001), and waveform modeling (e.g., Brandt et al., 2011; Moorkamp et al., 2019; Zhao et al., 1999). Four relevant body wave tomography studies are briefly summarized.

Fouch et al. (2004) used data from the Southern African Seismic Experiment (SASE) and Global Seismograph Network with the VanDecar (1991) inversion method to image the *P* and *S* wave velocity structure of the upper mantle across a SW-NE region of southern Africa. Their models revealed higher velocities beneath the Kaapvaal and Zimbabwe cratons, and lower velocities beneath the Bushveld Complex, Namaqua-Natal Belt, and Cape Fold Belt. Youssof et al. (2015) also used data from the SASE, and attempted to improve model resolution by employing finite-frequency sensitivity kernels in their travel time inversion. The Youssof et al. (2015) and Fouch et al. (2004) models are similar, and, in addition, similar to images of upper mantle structure beneath southern Africa obtained from surface wave tomography (e.g., Adams & Nyblade, 2011; Chevrot & Zhao, 2007; Fishwick, 2010; Li & Burke, 2006; Priestley et al., 2008).

In the northern part of our study area, Yu et al. (2016) and Mulibo and Nyblade (2013) also used body wave tomography methods to image upper mantle structure. Yu et al. (2016) used broadband seismic data from Botswana from the Seismic Arrays for African Rift Initiation experiment. They employed the method of Zhao et al. (1994) to invert travel times for upper mantle velocity structure, and obtained a model showing lower velocities beneath the ORZ, which they attributed to lithosphere thinned by incipient rifting. In the Mulibo and Nyblade (2013) study, *P* and *S* wave travel time residuals were inverted using the VanDecar (1991) method for upper mantle structure beneath the Damara Belt and other Proterozoic terranes in Zambia. In southern Zambia, they found a region of lower velocity in the upper mantle that extends much deeper into the mantle than the region of lower velocity beneath the ORZ imaged by Yu et al. (2016).

3. Data and Modeling

Data used in this study come from 153 stations belonging to six broadband seismic networks (SASE, doi: 10.7914/SN/XA_1997; Global Seismic Network, doi:10.7914/SN/II and doi: 10.7914/SN/IU; the temporary AfricaArray ZP network, doi: 10.7914/SN/ZP_2007; the Botswana Network of Autonomously Recording Seismographs, doi: 10.7914/SN/NR; the Seismic Arrays for African Rift Initiation network, doi: 10.7914/SN/XK_2012; and the permanent AfricaArray network, doi: 10.7914/SN/AF) that operated between 1997–1999 and 2010–2017 (Figure 1 and Table S1). Most of the data come from teleseismic earthquakes with $M \geq 5.5$ (Tables S2 and S3). A few *M* 5–5.4 Atlantic ridge events were included to improve azimuthal coverage from the W and NW. The *P* wave data set contains 10,848 travel times from 506 events, while the *S* wave data set contains 8,076 travel times from 449 events. Azimuthal coverage for both *P* and *S* waves is good (Figure S1).

The multichannel cross-correlation technique from VanDecar and Crosson (1990) was used to measure relative arrival times to 0.1 s for events well recorded on a minimum of five stations. A zero-phase band-pass filter with corner frequencies of 0.5 and 2 Hz for P waves and 0.04 to 0.2 Hz for *S* waves was applied to the

data prior to picking. Windows of 3 s for P and 12 s for *S* waves surrounding the picked phase arrival were used for the cross correlations.

VanDecar's (1991) method was used to invert the relative arrival times for a three-dimensional velocity model. In this method, slowness within the model domain is parameterized using splines under tension constrained at knots. The model extends from 8°S to 37°S and 10°E to 34°E, and extends downward 1,600 km from the surface. The model grid consists of 59 knots in latitude, 49 knots in longitude, and 42 knots in depth, with a total of 121,422 knots. Latitudinal and longitudinal node spacing is constant at half a degree. Radial nodes are spaced 20 km apart from the surface to a depth of 200 km, 33 km between 200-and 700-km depth, 50 km between 700- and 1,400-km depth, and 100 km between 1,400- and 1,600-km depth.

The inversion, performed using a one-dimensional starting model (IASP91; Kennett & Engdahl, 1991), results in a model of wave speed variations (VanDecar, 1991). Absolute V_p and V_s are not constrained by the method. The method simultaneously inverts for station terms, source terms, and slowness perturbations (VanDecar, 1991). The source terms account for structure outside the model and source mislocations. The station terms account for travel time variations arising from structure in the crust and uppermost mantle beneath stations where resolution is limited because of a lack of crossing rays. The inversion is underdetermined, and therefore, smoothing and damping parameters are used to obtain a model with the least amount of structure that fits the data. The smoothing parameter influences the sharpness of the anomaly boundaries while the damping parameter influences the anomaly amplitudes. The effects of the parameters have been explored using trade-off curves, with parameters in the elbow of the curves selected for the final model (Figure S2). The final *P* wave model accounts for 87.5% of the *P* wave RMS initial misfit, and the final *S* wave model accounts for 89.5% of the *S* wave RMS initial misfit.

The absolute values of the station terms for the P and *S* wave models are, on average, ~0.25–1.5 s (Figure S3). Similar ranges of station terms have been reported for eastern and southern Africa by others using the VanDecar inversion method (Fouch et al., 2004; Mulibo & Nyblade, 2013; Park & Nyblade, 2006; Ritsema et al., 1998).

4. Model Results and Resolution

Results of the *P* and *S* wave inversions are shown in map view (Figure 2) and in depth slices (Figures 3 and S4). The *P* and *S* models are similar. From south to north, the models show a region of lower velocities beneath the Cape Fold Belt (δV_p = ~−0.3%, δV_s = ~−0.5%), a region of higher velocities beneath the Namaqua-Natal Belt, Kaapvaal and Zimbabwe cratons, and parts of the Limpopo Belt (δV_p = ~0.3–0.5%, δV_s = ~0.5–0.8%), a region of lower velocities beneath the Bushveld Complex, and parts of the Limpopo Belt (δV_p = ~−0.4%, δV_s = ~−0.6%), with this region extending to the northwest beneath parts of the Okwa Terrane and Magondi Belt (δV_p = ~−0.4%, δV_s = ~−0.6%) in northern South Africa and southern Botswana. To the west and northwest beneath the Rehoboth Province, the Okwa Terrane, and the Magondi Belt, a region of higher velocities is present (δV_p = ~0.3–0.5%, δV_s = ~0.5–0.8%). Further to the northwest beneath the Damara-Ghanzi-Chobe Belt, and also beneath the ORZ, regions of lower velocity are present (δV_p = ~−0.5%, δV_s = ~−0.8%). In the northernmost part of the model, a pronounced low-velocity region is present beneath southwestern Zambia that extends to the northeast into northern Zambia (δV_p = ~−0.4–0.8%, δV_s = ~−0.6–1.0%).

Model resolution has been evaluated using checkerboard and tabular body tests. The checkers are composed of alternating positive and negative 200-km-diameter spherical (±5%) velocity anomalies (Figures S5c–S5e). The tabular bodies have a 5% velocity reduction (Figures S6a–S6c). Synthetic travel times were generated for the input models using the actual raypaths, with random noise added to the arrival times (zero mean and 0.04-s standard deviation for P waves and zero mean and 0.05-s standard deviation for *S* waves). The synthetic travel times were inverted for velocity structure using the same model parameters, including smoothing and damping, as used in the inversion with the observed data.

Figures 4 and S5 show recovered checkerboard models with rows of 200-km-diameter input checkers centered at depths of 100 to 800 km, along with west-east vertical slices through one row of the recovered checkers. Good lateral resolution is found at depths of 200 to 600 km, where the lateral boundaries of the checkers are well recovered for both the *P* and *S* wave models. The regions of northern South Africa,

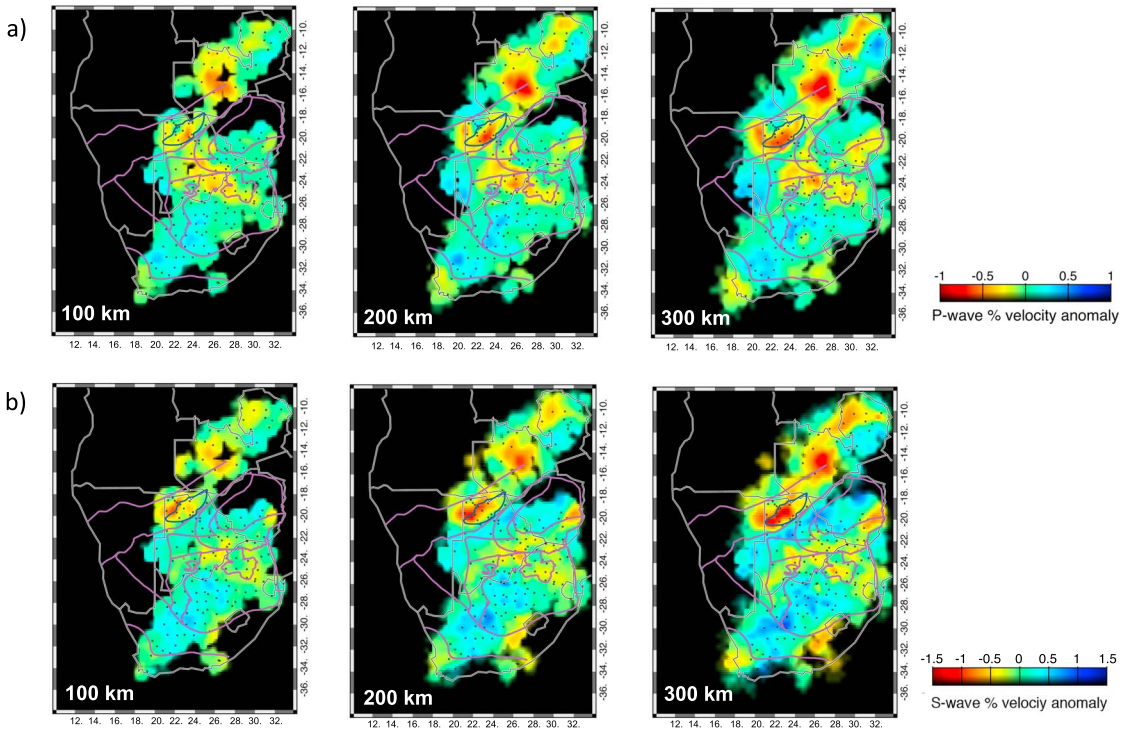

Figure 2. (a) Horizontal cross sections through the *P* wave tomography model at depths of 100, 200, and 300 km. (b) Horizontal cross sections through the *S* wave tomography model at depths of 100, 200, and 300 km. The purple lines denote the Precambrian terrane boundaries shown in Figure 1 and the blue line denotes the Okavango rift. Small black dots show seismic station locations. Areas with hit counts of 3 or less are shown in black.

northern Namibia, southern Zimbabwe, and Botswana have the best resolution because of denser station spacing. Vertical cross sections with checkers centered at 200-km depth, as well as the tabular body tests (Figure S6), illustrate that there is over 100 km of vertical smearing and hence limited depth resolution in the models (i.e., the bottom of input checkers at 300-km depth smears to ~400-km depth).

5. Discussion

New features in our model that advance our understanding of the structure and composition of the southern African upper mantle include the region of higher velocities beneath the Rehoboth Province and parts of the Magondi Belt and Okwa Terrane, a region of lower velocities beneath the Damara-Ghanzi-Chobe Belt and ORZ, and regions of lower velocities that extend to the north and northwest from the Bushveld Complex beneath parts of the Magondi Belt, Okwa Terrane, and Limpopo Belt (Figures 2 and 3). In areas where our model overlaps geographically with other body and surface wave models, there is good agreement in the first-order model features. The velocity variations seen in our model beneath regions spanning the SASE network are almost identical to the models published by Fouch et al. (2004) and Youssof et al. (2015). In northwestern Botswana, our model shows upper mantle structure beneath the Okavango rift similar to the Yu et al. (2016) model, and in Zambia, upper mantle structure in our model is almost indistinguishable from structure in the Mulibo and Nyblade (2013) model.

We use our results to first address the geographic extent of the greater Kalahari Craton, as defined by regions of thicker lithosphere. In comparison to upper mantle velocities found beneath the Kaapvaal and Zimbabwe cratons, the higher velocities beneath parts of the Rehoboth Province, Magondi Belt, and Okwa Terrane indicate that thick cratonic lithosphere may extend well to the west and northwest of the Kaapvaal and Zimbabwe cratons. Further to the northwest beneath the Damara-Ghanzi-Chobe Belt is a region of lower upper mantle velocities, which also includes the ORZ. If the edge of thick cratonic lithosphere lies along the boundary between the Damara-Ghanzi-Chobe Belt and the Rehoboth Province, then the lower upper mantle velocities beneath the Damara-Ghanzi-Chobe Belt can be attributed to thinner off-craton

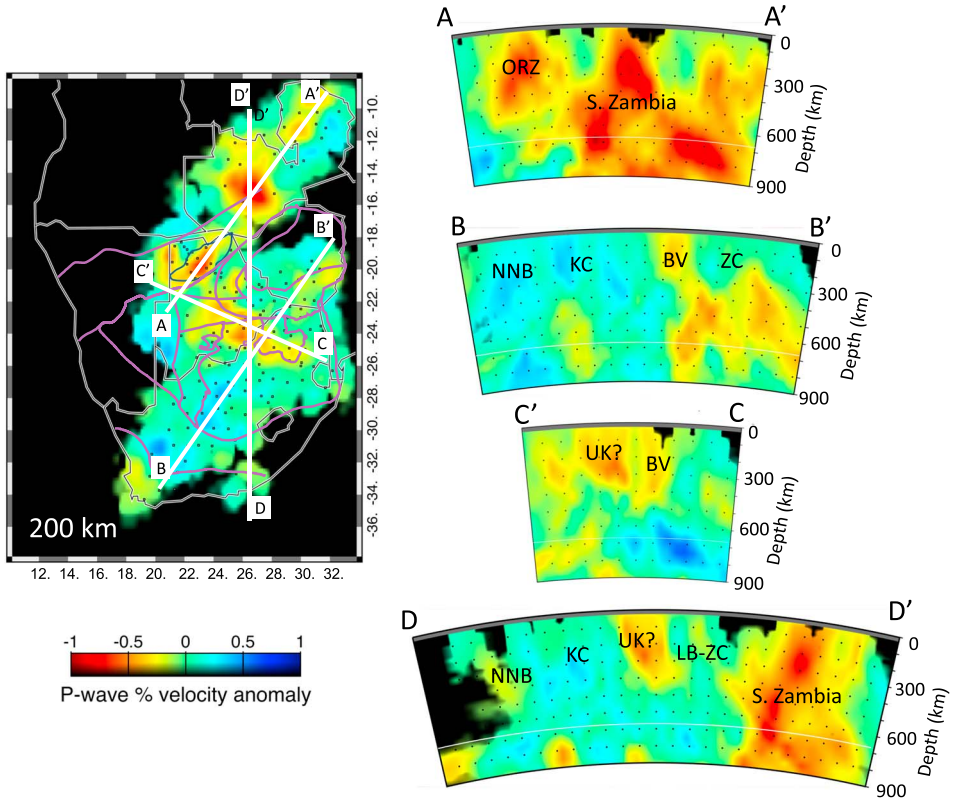

Figure 3. Vertical cross sections through the *P* wave model illustrating the velocity structure found beneath many of the Precambrian terranes and Okavango Rift. BV = Bushveld Complex, KC = Kaapvaal Craton, LB-ZC = Limpopo Belt and Zimbabwe Craton, NNB = Namaqua-Natal Belt, ORZ = Okavango Rift Zone, UK? = region of lower velocities attributed to the Bushveld and/or Umkondo magmatic events. S. Zambia = deep-seated region of lower velocities beneath southern Zambia that may extend into the mantle transition zone. Areas with hit counts of 3 or less are shown in black.

lithosphere. This interpretation is consistent with models of magnetotelluric data. Khoza et al. (2013) and Muller et al. (2009) reported a lithospheric thickness of ~160 km for the Damara-Ghanzi-Chobe Belt, which compares to a lithospheric thickness of ~200–225 km beneath much of the Kalahari Craton (Adams & Nyblade, 2011; Fishwick, 2010; Priestley et al., 2008).

However, Yu et al. (2016) attributed the region of lower velocities under the ORZ to a rift-related thermal anomaly and not the edge of the cratonic lithosphere. It is possible that the lower velocities beneath the Damara-Ghanzi-Chobe Belt could reflect thinner off-craton lithosphere as well as a thermal perturbation to the upper mantle related to rifting. While model resolution of upper mantle structure under the Damara-Ghanzi-Chobe Belt away from the ORZ is limited, our model does show that the region of lower velocities extends beyond the ORZ proper to the northwest (Figure 2). This finding suggests that the lower velocities may not result entirely from the thermal contribution of rifting, and that instead at least part of the decrease in velocity could be caused by thinner off-craton lithosphere. We therefore favor an interpretation that places the edge of the greater Kalahari Craton lithosphere along the boundary between the Damara-Ghanzi-Chobe Belt and the Rehoboth Province, and that ascribes the region of lower velocities under the ORZ to both a thermal component of rifting and the presence of thinner off-craton lithosphere.

Comparing upper mantle structure beneath the ORZ and Damara-Ghanzi-Chobe Belt with structure beneath southern Zambia further supports an interpretation that the craton margin lies along the boundary between the Damara-Ghanzi-Chobe Belt and Rehoboth Province. Figures 3 and S4 show vertical slices through the models. In these figures, the region of lower velocities in southern Zambia appears even larger and extends to greater depths than beneath the ORZ, possibly as deep as the mantle transition zone. The greater depth extent of the southern Zambia anomaly is supported by the tabular body resolution tests (Figure S6), as well as by similar tests in Mulibo and Nyblade (2013). An anomaly under the northern part of

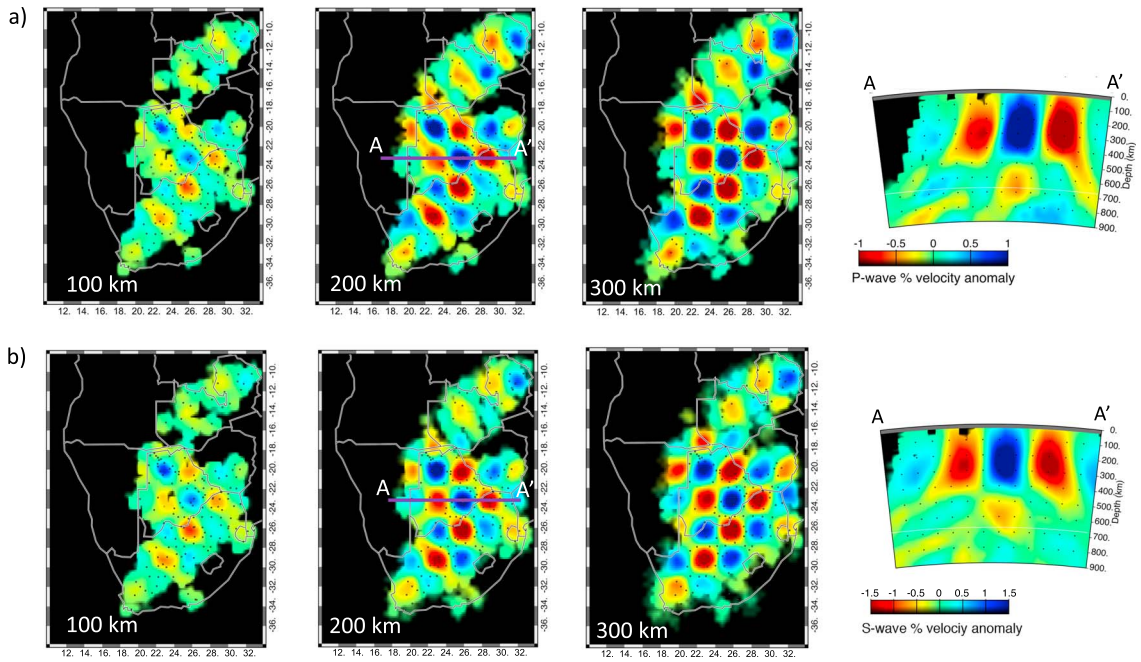

Figure 4. (a) Checkerboard resolution test results for the *P* wave tomography model at depths of 100, 200, and 300 km. (b) Checkerboard resolution test results for the *S* wave tomography model at depths of 100, 200, and 300 km. The input model is described in the text. Small black dots show seismic station locations. Areas with hit counts of 3 or less are shown in black.

the Damara Belt in southern Zambia possibly extending as deep as the transition zone strongly indicates that thick cratonic lithosphere does not extend further to the northeast of either the Rehoboth Province or Zimbabwe Craton.

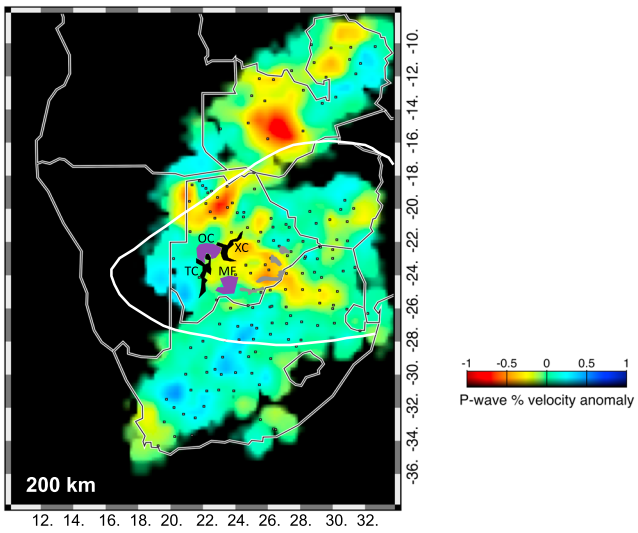

Figure 5. Map showing *P* wave tomography model at 200-km depth, the outline of the 1.1-Ga Umkondo Large Igneous Province (white line), two mafic/ultramafic complexes (TC = Tshane Complex, XC = Xade Complex; black regions), and several regions of mafic lavas in southeastern Botswana (grey regions) that are part of the Umkondo magmatic province (after Hanson et al., 2004), and two complexes that are the same age as the Bushveld Complex (MF = Malopo Farms Complex, OC = Okwa Complex; purple regions; after Mapeo et al., 2006). Areas with hit counts of 3 or less are shown in black.

Regarding the regions of lower velocities that extend to the north and northwest from the Bushveld Complex beneath parts of the Magondi Belt, Okwa Terrane, and Limpopo Belt, it is unlikely that they result from thermal anomalies because no Phanerozoic tectonism has affected these terranes (Begg et al., 2009). Instead, following the interpretation of Fouch et al. (2004) for the lower velocities beneath the Bushveld Complex, we attribute the lower velocities beneath those terranes to compositionally modified lithospheric mantle from large magmatic events. Fouch et al. (2004) invoked compositional fertilization (i.e., iron enrichment) of the lithospheric mantle at the time of intrusion of Bushveld magmas to explain the lower velocities under the Bushveld Complex, noting that refertilized cratonic mantle rocks have normative seismic velocities up to 1% lower than depleted nodular peridotites (Jordan, 1979).

The Bushveld Complex extends as far west as the Malopo Farms complex in southern Botswana (Figures 1, 3, and 5) and also as far to the northwest as the Okwa Complex (Figure 5; Mapeo et al., 2004, 2006; Singletary et al., 2003; Cawthorn et al., 2006). Therefore, one possibility is that the mantle lithosphere in regions with lower velocities in southeastern and central Botswana, as well as in the Limpopo Belt, was modified by the Bushveld magmatic event. The slightly larger amplitude of these low-velocity anomalies in the *P* wave model compared to the *S* wave model could also indicate metasomatic alteration of the cratonic lithosphere (Schutt & Lesher, 2010), but could as well simply result from the regularization parameters used in the inversion.

In addition to the Bushveld event, several other large Precambrian magmatic events occurred in southern Africa. Relics of one of them, the 1.1-Ga Umkondo event, include mafic/ultramafic intrusions (Tshane and Xade Complexes; Figure 5) in central Botswana and flows of mafic lava in southeastern Botswana and northwestern South Africa (Corner & Durrheim, 2018; de Kock et al., 2014; Hanson et al., 2004) where the lower velocities are found (Figures 3 and 5). Fadel et al. (2018) suggest that the composition of the crust in these areas may also have been modified. Thus, a second possibility is that the lower velocities beneath parts of the Magondi Belt, Okwa Terrane, and Limpopo Belt may result from mantle lithosphere modified by the Umkondo magmatic event. Given the spatial overlap between the regions of lower velocity and regions of Bushveld and Umkondo magmatism, it is likely that the Kalahari Craton mantle lithosphere was modified by Proterozoic magmatic events over a much larger region than recognized.

6. Summary and Conclusions

New broadband seismic data have been combined with data from permanent seismic stations and previous temporary stations to develop *P* and *S* wave velocity models of the upper mantle beneath southern Africa. Features in the model not imaged in previous models include (1) regions of higher velocities beneath the Rehoboth Province and northern parts of the Okwa Terrane and the Magondi Belt, (2) regions of lower velocities beneath the Damara-Ghanzi-Chobe Belt and ORZ, and (3) regions of lower velocities extending to the north and northwest of the Bushveld Complex into southern parts of the Okwa Terrane, Magondi Belt, and Limpopo Belt. We attribute the higher velocities beneath the Rehoboth Province and parts of the northern Okwa Terrane and the Magondi Belt to thick cratonic lithosphere. The region of lower velocities beneath the Damara-Ghanzi-Chobe Belt and ORZ we attribute to thinner off-craton lithosphere that may also have experienced some thermal alteration under the Okavango Rift. Combined, these interpretations suggest that the northern edge of the greater Kalahari Craton lithosphere lies along the southern boundary of the Damara-Ghanzi-Chobe Belt. The lower velocity regions to the north and northwest of the Bushveld Complex beneath parts of the Okwa Terrane, Magondi Belt, and Limpopo Belt we argue may represent regions of mantle lithosphere modified by the 2.05-Ga Bushveld and/or 1.1-Ga Umkondo magmatic events.

Acknowledgments
This work was supported by grant ALW-GO-AO/11-30 provided by Nederlandse Organisatievoor Wetenschappelijk Onderzoek (NWO) and National Science Foundation grants 0440032, 0530062, 0824781, 1128936, and 1634108. We acknowledge the efforts of Arie van Wettum from Utrecht University and colleagues at the Botswana Geological Survey for installing and maintaining the NARS-Botswana network, and thank two anonymous reviewers for helpful and constructive reviews. Data used in this study can be obtained from the IRIS data management center (http://ds.iris.edu/ds/).

References

Adams, A., & Nyblade, A. (2011). Shear wave velocity structure of the southern African upper mantle with implications for the uplift of southern Africa. *Geophysical Journal International*, *186*(2), 808–824. https://doi.org/10.1111/j.1365-246X.2011.05072.x

Begg, G. C., Griffin, W. L., Natapov, L. M., O'Reilly, S. Y., Grand, S. P., O'Neill, C. J., et al. (2009). The lithospheric architecture of Africa: Seismic tomography, mantle petrology, and tectonic evolution. *Geosphere*, *5*(1), 23–50. https://doi.org/10.1130/GES00179.1

Brandt, M., Grand, S., Nyblade, A., & Dirks, P. (2011). Upper mantle seismic structure beneath southern Africa: Constraints on the buoyancy supporting the African Superswell. *Pure and Applied Geophysics*, *169*(4), 595–614. https://doi.org/10.1007/s00024-011-0361-8

Carlson, R. W., Boyd, F. R., Shirey, S. B., Janney, P. E., Grove, T. L., Bowring, S. A., et al. (2000). Continental growth, preservation and modification in southern Africa. *GSA Today*, *20*, 1–7.

Cawthorn, R. G., Eales, H. V., Walraven, F., Uken, R., & Watkeys, M. K. (2006). The Bushveld complex. In M. R. Johnson, C. R. Anhaeusser, & R. J. Thomas (Eds.), *The Geology of South Africa*, (pp. 261–281). Johannesburg, South Africa: Geol. Soc. of S. Afr.

Chevrot, S., & Zhao, L. (2007). Multiscale finite-frequency Rayleigh wave tomography of the Kaapvaal craton. *Geophysical Journal International*, *169*(1), 201–215. https://doi.org/10.1111/j.1365-246X.2006.03289.x

Cornell, D. H., Thomas, R. J., Moen, H. F. G., Reid, D. L., Moore, J. M., & Gibson, R. L. (2006). The Namaqua-Natal province. In M. R. Johnson, C. R. Anhaeusser, & R. J. Thomas (Eds.), *The geology of South Africa*, (pp. 325–379). Johannesburg, South Africa: Geol. Soc. of S. Afr.

Corner, B., & Durrheim, R. (2018). An integrated geophysical and geological interpretation of the southern African lithosphere. In S. Siegesmund, et al. (Eds.), *Geology of Southwest Gondwana, Regional Geology*, (pp. 19–71, Reviews). https://doi.org/10.1007/978-3-319-68920-3_2

De Kock, M. O., Ernst, R., Soderlund, U., Jourdan, F., Hofmann, A., Le Gall, B., et al. (2014). Dykes of the 1.11 Ga Umkondo LIP, Southern Africa: Clues to a complex plumbing system. *Precambrian Research*, *249*, 129–143. https://doi.org/10.1016/j.precamres.2014.05.006

de Wit, M. J., Roering, C., Hart, R. J., Armstrong, R. A., Ronde, C. E. J., Green, R. W. E., et al. (1992). Formation of an Archaean continent. *Nature*, *357*(6379), 553–562. https://doi.org/10.1038/357553a0

Dirks, P. H. G. M., & Jelsma, H. A. (2002). Crust-mantle decoupling and the growth of the Archaean Zimbabwe Craton. *Journal of African Earth Sciences*, *34*(3-4), 157–166. https://doi.org/10.1016/S0899-5362(02)00015-5

Eglington, B. M., & Armstrong, R. A. (2004). The Kaapvaal Craton and adjacent orogens, southern Africa: A geochronological database and overview of the geological development of the craton. *South African Journal of Geology*, *107*(1-2), 13–32. https://doi.org/10.2113/107.1-2.13

Fadel, I., van der Meijde, M., & Paulssen, H. (2018). Crustal structure and dynamics of Botswana. *Journal of Geophysical Research: Solid Earth*, *123*(12), 10,659–10,671. https://doi.org/10.1029/2018JB016190

Fishwick, S. (2010). Surface wave tomography: Imaging of the lithosphere-asthenosphere boundary beneath central and Southern Africa. *Lithos*, *120*(1-2), 63–73. https://doi.org/10.1016/j.lithos.2010.05.011

Fouch, M. J., James, D. E., VanDecar, J. C., & van der Lee, S. (2004). The Kaapvaal Seismic Group, (2004), Mantle seismic structure beneath the Kaapvaal and Zimbabwe cratons. *South African Journal of Geology*, *107*(1-2), 33–44. https://doi.org/10.2113/107.1-2.33

Grégoire, M., Tinguely, C., Bell, D. R., & Le Roex, A. P. (2005). Spinel lherzolite xenoliths from the Premier kimberlite (Kaapvaal craton, South Africa): Nature and evolution of the shallow upper mantle beneath the Bushveld complex. *Lithos*, *84*(3-4), 185–205. https://doi.org/10.1016/j.lithos.2005.02.004

Griffin, W., O'Reilly, S., Natapov, L., & Ryan, C. (2003). The evolution of lithospheric mantle beneath the Kalahari Craton and its margins. *Lithos*, *71*(2-4), 215–241. https://doi.org/10.1016/j.lithos.2003.07.006

Hansen, S., Nyblade, A., Julia, J., Dirks, P., & Durrheim, R. (2009). Upper-mantle low velocity zone structure beneath the Kaapvaal craton from *S*-wave receiver functions. *Geophysical Journal International*, *178*(2), 1021–1027. https://doi.org/10.1111/j.1365-246X.2009.04178.x

Hanson, R. E., Crowley, J. L., Bowring, S. A., Ramezani, J., Gose, W. A., Dalziel, I. W. D., et al. (2004). Coeval large-scale magmatism in the Kalahari and Laurentian cratons during Rodinia assembly. *Science*, *304*(5674), 1126–1129. https://doi.org/10.1126/science.1096329

Hartnady, C., Joubert, P., & Stowe, C. (1985). Proterozoic crustal evolution in southwestern Africa. *Episodes*, *8*, 236–243.

Jordan, T. H. (1979). Mineralogies, densities and seismic velocities of garnet lherzolites and their geophysical implications. In F. R. Boyd, & H. O. A. Meyer (Eds.), *The mantle sample: Inclusions in kimberlites and other volcanics Proceedings of the second international kimberlite conference*, (pp. 1–14). Washington, D.C., United States: American Geophysical Union. https://doi.org/10.1029/SP016p0001

Kennett, B., & Engdahl, E. (1991). Traveltimes for global earthquake location and phase identification. *Geophysical Journal International*, *122*, 429–465.

Kgaswane, E. M., Nyblade, A. A., Julia, J., Dirks, P. H. G. M., Durrheim, R. J., & Pasyanos, M. E. (2009). Shear wave velocity structure of the lower crust in southern Africa: Evidence for compositional heterogeneity within Archaean and Proterozoic terrains. *Journal of Geophysical Research*, *114*(B12), B12304. https://doi.org/10.1029/2008JB006217

Khoza, T. D., Jones, A. G., Muller, M. R., Evans, R. L., Miensopust, M. P., & Webb, S. J. (2013). Lithospheric structure of an Archean craton and adjacent mobile belt revealed from 2-D and 3-D inversion of magnetotelluric data: Example from southern Congo craton in northern Namibia. *Journal of Geophysical Research: Solid Earth*, *118*, 4378–4397. https://doi.org/10.1002/jgrb.50258

Kinabo, B. D., Hogan, J. P., Atekwana, E. A., Abdelsalam, M. G., & Modisi, M. P. (2008). Fault growth and propagation during incipient continental rifting: Insights from a combined aeromagnetic and Shuttle Radar Topography Mission digital elevation model investigation of the Okavango Rift Zone, northwest Botswana. *Tectonics*, *27*, TC3013. https://doi.org/10.1029/2007TC002154

Kröner, A., & Stern, R. (2004). Africa: Pan-african orogeny. In *Encyclopedia of Geology*, (pp. 1–12). Elsevier.

Li, A., & Burke, K. (2006). Upper mantle structure of southern Africa from Rayleigh wave tomography. *Journal of Geophysical Research*, *111*(B10), B10303. https://doi.org/10.1029/2006JB004321

Mapeo, R., Kampunzu, A., Ramokate, L., Corfu, F., & Key, R. (2004). Bushveld-age magmatism in southeastern Botswana, evidence from U-Pb zircon and titanite geochronology of the Moshaneng Complex. *South African Journal of Geology*, *107*, 219–232.

Mapeo, R., Ramokate, L., Corfu, F., Davis, D., & Kampunzu, A. (2006). The Okwa basement complex, western Botswana: U-Pb zircon geochronology and implications for Eburnean processes in southern Africa. *Journal of African Earth Sciences*, *46*(3), 253–262. https://doi.org/10.1016/j.jafrearsci.2006.05.005

Modisi, M. P., Atekwana, E. A., Kampunzu, A. B., & Ngwisanyi, T. H. (2000). Rift kinematics during the incipient stages of continental extension: Evidence from the nascent Okavango rift basin, northwest Botswana. *Geology*, *28*(10), 939–942. https://doi.org/10.1130/0091-7613(2000)28<939:RKDTIS>2.0.CO;2

Moorkamp, M., Fishwick, S., Walker, R. J., & Jones, A. G. (2019). Geophysical evidence for crustal and mantle weak zones controlling intra-plate seismicity—The 2017 Botswana earthquake sequence. *Earth and Planetary Science Letters*, *506*, 175–183. https://doi.org/10.1016/j.epsl.2018.10.048

Mulibo, G., & Nyblade, A. (2013). The *P* and *S* wave velocity structure of the mantle beneath eastern Africa and the African superplume anomaly: Mantle structure beneath Eastern Africa. *Geochemistry, Geophysics, Geosystems*, *14*, 2696–2715. https://doi.org/10.1002/ggge.20150

Muller, M. R., Jones, A., Evans, R., Grütter, H. S., Hatton, C., Garcia, X., et al. (2009). Lithospheric structure, evolution and diamond prospectivity of the Rehoboth Terrane and western Kaapvaal Craton, southern Africa: Constraints from broadband magnetotellurics. *Lithos*, *112*, 93–105. https://doi.org/10.1016/j.lithos.2009.06.023

Nguuri, T. K., Gore, J., James, D. E., Webb, S. J., Wright, C., Zengeni, T. G., et al., & Kaapvaal Seismic Group (2001). Crustal structure beneath southern Africa and its implications for the formation and evolution of the Kaapvaal and Zimbabwe cratons. *Geophysical Research Letters*, *28*(13), 2501–2504. https://doi.org/10.1029/2000GL012587

Park, Y., & Nyblade, A. A. (2006). *P*-wave tomography reveals a westward dipping low velocity zone beneath the Kenya Rift. *Geophysical Research Letters*, *33*, L07311. https://doi.org/10.1029/2005GL025605

Priestley, K., McKenzie, D., Debayle, E., & Pilidou, S. (2008). The African upper mantle and its relationship to tectonics and surface geology. *Geophysical Journal International*, *175*(3), 1108–1126. https://doi.org/10.1111/j.1365-246X.2008.03951.x

Reichhardt, F. J. (1994). The Molopo Farms Complex, Botswana: History, stratigraphy, petrography, petrochemistry and Ni–Cu–PGE mineralization. *Exploration and Mining Geology*, *3*, 263–284.

Richardson, S. H., & Shirey, S. B. (2008). Continental mantle signature of Bushveld magmas and coeval diamonds. *Nature*, *453*(7197), 910–913. https://doi.org/10.1038/nature07073

Ritsema, J., Nyblade, A. A., Owens, T. J., & Langston, C. A. (1998). Upper mantle seismic velocity structure beneath Tanzania: Implications for the stability of cratonic lithosphere. *Journal of Geophysical Research*, *103*(B9), 21,201–21,213. https://doi.org/10.1029/98JB01274

Schutt, D. L., & Lesher, C. E. (2010). Compositional trends among Kaapvaal Craton garnet peridotite xenoliths and their effects on seismic velocity and density. *Earth and Planetary Science Letters*, *300*(3-4), 367–373. https://doi.org/10.1016/j.epsl.2010.10.018

Singletary, S. J., Hanson, R. E., Martin, M. W., Crowley, J. L., Bowring, S. A., Key, R. M., et al. (2003). Geochronology of basement rocks in the Kalahari desert, Botswana, and implications for regional Proterozoic tectonics. *Precambrian Research*, *121*, 47–71.

Thomas, R., von Veh, M., & McCourt, S. (1993). The tectonic evolution of southern Africa: An overview. *Journal of African Earth Sciences*, *16*(1-2), 5–24. https://doi.org/10.1016/0899-5362(93)90159-N

Van Schijndel, V., Cornell, D. H., Hoffmann, K.-H., & Frei, D. (2011). Three episodes of crustal development in the Rehoboth Province, Namibia. In D. J. J. Van Hinsbergen, S. J. H. Buiter, T. H. Torsvik, C. Gaina, & S. J. Webb (Eds.), *The formation and evolution of Africa: A synopsis of 3.8 Ga of Earth history*, (Vol. 357, pp. 27–47). Geological Society, London: Special Publications.

VanDecar, J., & Crosson, R. (1990). Determination of teleseismic relative phase arrival times using multi-channel cross-correlation and least squares. *Bulletin of Seismological Society of America*, *80*, 150–169.

VanDecar, J. C. (1991). *Upper mantle structure of the Cascadia subduction zone from nonlinear teleseismic travel time inversion*, Ph. D. Thesis. Seattle, WA: University of Washington.

Viljoen, F., Dobbe, R., & Smit, B. (2009). Geochemical processes in peridotite xenoliths from the Premier diamond mine, South Africa: Evidence for the depletion and refertilisation of subcratonic lithosphere. *Lithos*, *112S*, 1133–1142.

Webb, S. J., Cawthorn, R. G., Nguuri, T. K., & James, D. E. (2004). Gravity modeling of Bushveld complex connectivity supported by Southern African Seismic Experiment results. *South African Journal of Geology*, *107*(1-2), 207–218. https://doi.org/10.2113/107.1-2.207

Youssof, M., Thybo, H., Artemieva, I., & Levander, A. (2015). Upper mantle structure beneath southern African cratons from seismic finite-frequency *P*- and *S*-body wave tomography. *Earth and Planetary Science Letters*, *420*, 174–186. https://doi.org/10.1016/j.epsl.2015.01.034

Yu, Y., Liu, K. H., Huang, Z., Zhao, D., Reed, C. A., Moidaki, M., et al. (2016). Mantle structure beneath the incipient Okavango rift zone in southern Africa. *Geosphere*, *13*(1), 102–111. https://doi.org/10.1130/GES01331.1

Zhao, D., Hasegawa, A., & Kanamori, H. (1994). Deep structure of Japan subduction zone as derived from local, regional, and teleseismic events. *Journal of Geophysical Research*, *99*(B11), 22,313–22,329. https://doi.org/10.1029/94JB01149

Zhao, M., Langston, C., Nyblade, A., & Owens, T. (1999). Upper mantle velocity structure beneath southern Africa from modeling regional seismic data. *Journal of Geophysical Research*, *104*(B3), 4783–4794. https://doi.org/10.1029/1998JB900058